Hindawi
Advances in Materials Science and Engineering
Volume 2019, Article ID 9290318, 10 pages
https://doi.org/10.1155/2019/9290318

Research Article

Experimental Investigation of the Anchoring Effect of Two Different Types of Rock Bolts on Fractured Rock

Rongchao Xu[1] **and Hui Zhou**[2]

[1]*College of Geosciences and Engineering, North China University of Water Resources and Electric Power, Zhengzhou, Henan 450046, China*
[2]*State Key Laboratory of Geomechanics and Geotechnical Engineering, Institute of Rock and Soil Mechanics, Chinese Academy of Sciences, Wuhan, Hubei 430071, China*

Correspondence should be addressed to Rongchao Xu; rcxirsm@126.com

Received 19 December 2018; Revised 2 January 2019; Accepted 27 January 2019; Published 19 February 2019

Academic Editor: Carlo Santulli

A deep understanding of the anchoring effect of rock bolts on fractured rock is essential for support design in rock engineering. In this paper, cubic specimens containing a single preexisting flaw with different inclination angles were made by high-strength gypsum; uniaxial compression tests were conducted on bolted and unbolted specimens to study the anchoring effect of the fully bonded bolt and the prestressed bolt on fractured rock. The mechanical parameters and failure characteristics of bolted and unbolted specimens were compared and analyzed in detail. The results indicated that both the prestressed and fully bonded bolt had a significant influence on the mechanical behavior of fractured rock. The average value of E, σ_i, σ_p, and σ_r of bolted specimens all increased due to the effect of the rock bolt. The increase degree was the greatest for the specimens with flaw inclination angle of 45°. The increase in residual strength, σ_r, was the most significant among all the mechanical parameters. The mechanical parameters of specimens anchored with a prestressed bolt increased with an increase in pretension stress. Besides, the reinforcement effect of the two types of rock bolts was different for different mechanical parameters. The bolted specimens displayed different failure characteristics compared to the unbolted specimens. Variation of tension stress in the prestressed bolt during the loading process was divided into three different stages. With an increase in the inclination angle from 30° to 60°, the peak tension stress value first increased and then decreased and obtained the maximum value at inclination angle of 45°. Besides, the peak tension stress value increased with pretension stress.

1. Introduction

Cracks usually initiate from the tips of preexisting flaws, joints, and other weak planes after rock excavation. The propagation and coalescence of these new cracks pose a great threat to the stability of the surrounding rock. Rock bolting is one of the most commonly used means of supporting in rock engineering to stabilize the ground and ensure safe working conditions [1]. The fully bonded bolt and the prestressed bolt are the most widely used rock bolts in civil and mining engineering due to their effectiveness and applicability. In recent years, new types of rock bolts, such as the cone bolt [2, 3], the Durabar [4], the D-bolt [5–7], and other energy-absorbing bolts [8, 9], have been developed to solve the issue of rock burst, which usually cause serious damage to on-site construction and pose a considerable threat to on-site workers in deep rock engineering because of the great amount of energy release [10–16].

A deep understanding of the working mechanism and anchoring effect of rock bolts is essential for support design in rock engineering. As such, extensive research studies have been conducted to address this problem in the past several decades using theoretical analysis [17–19], laboratory experiments [20–24], and numerical modeling [1, 25, 26]. The support loads to the rock mass provided by a fully bonded bolt develop gradually when rock deforms [27]. On the other hand, the prestressed bolts are installed with a certain pretension stress. Due to the effect of pretension stress, the

prestressed bolts can provide support pressure to the surrounding rock immediately after installation. The anchoring effect of the two types of bolts is generally different due to the significant differences in their working mechanisms. Although the abovementioned studies have advanced our understanding of the working mechanisms and anchoring effects of rock bolts, the different anchoring effects of fully bonded and prestressed bolts on fractured rock have rarely been studied.

The aim of this experimental research is to study the anchoring effect of the fully bonded bolt and the prestressed bolt on fractured rock. Cubic specimens containing a single preexisting flaw with different inclination angles were made by high-strength gypsum. Uniaxial compression tests were conducted on bolted and unbolted specimens. The mechanical parameters and failure characteristics of bolted and unbolted specimens were compared and analyzed in detail. These research results are expected to provide useful guidance for support design in rock engineering.

2. Specimen Preparation and Testing Program

2.1. Specimen Preparation. The specimens were made from a mixture of high-strength gypsum, water, and quartz sand in a ratio of 3 : 1 : 0.5 by weight. Rectangular prismatic specimens, with dimensions of 120 × 60 × 40 mm (height × width × thickness), were prepared. The physical and mechanical parameters of the intact specimen (with no preexisting flaws) are given in Table 1. The preexisting flaw with different inclination angles (30°, 45°, and 60°) was made in the specimen by inserting a sheet of resin flake with a thickness of 0.2 mm and length of 20 mm during the specimen's solidification period (Figure 1(a)). All specimens were cured at room temperature condition for 28 days before the experimental tests.

A steel bar (70 mm in length and 4 mm in diameter) with elastic modulus of 200 GPa was used to simulate the rock bolt in this experiment (Figure 1(b)). A resistance strain gage was bonded to the steel bar to exactly measure the applied pretension stress and the variation of tension stress in the test. To apply the pretension stress, a spanner was used to tighten the nut which was set at the end of the bar. A bolt plate with dimensions of 35 × 35 × 2 mm (length × width × thickness) was also placed at each end of the steel bar to better simulate the real working conditions of the rock bolt.

A circular hole with a diameter of approximately 4.3 mm was drilled in the central position across the flaw to install the bolt into the sample. An anchoring agent which was a mixture of high-strength gypsum and water at a mass ratio of 3 : 1 was used to bond the steel bar and the borehole wall to simulate the fully bonded and untensioned rock bolt (Figure 1(c)). On the other hand, the steel bar was unbonded from the borehole and a certain pretension stress value was applied to simulate the prestressed rock bolt (Figure 1(d)).

2.2. Testing System and Program. The uniaxial compression tests were conducted with the RMT-150C rock mechanics servo-controlled testing system in Institute of Rock and Soil Mechanics, Chinese Academy of Sciences. The axial and lateral strains were measured by LVDT. The AEs during the compression tests were monitored with a 16-channel PAC-DISP system, and crack propagation process was recorded by a high-speed camera (Figure 2). The axial load was applied at a rate of 0.002 mm/s. Twelve groups of uniaxial compression tests under different test conditions were conducted, as listed in Table 2, and three samples were tested for each group.

Table 1: Physical and mechanical parameters of the intact sample.

Uniaxial compressive strength (MPa)	Elastic modulus (GPa)	Tensile strength (MPa)	Dry density ($g \cdot cm^{-3}$)	Poisson ratio
39.27	13.46	1.48	1.83	0.23

3. Test Results

3.1. Typical Stress-Strain Curves and Mechanical Parameters. Typical stress-strain curves for the bolted and unbolted specimens under uniaxial compression are shown in Figure 3, which indicates that both the prestressed and fully bonded bolt had a significant influence on the mechanical behavior of fractured rock. The stress-strain curves of the bolted specimens possessed distinctive characteristics as compared with the unbolted specimens due to the effect of the bolt, which are summarized as follows:

(1) Both the uniaxial compressive strength and residual strength were improved for the bolted specimens. Besides, the uniaxial compressive strength for the specimens anchored with the prestressed bolt increased with the pretension stress value.

(2) The drop rate of axial stress significantly reduced after peak strength for bolted specimens. While the axial stress dropped drastically to a low value (even to 0) after peak strength for the unbolted samples.

(3) Lateral deformation was significantly inhibited after peak strength, especially for the samples containing flaws with inclination angles of 30° (Figure 3(a)) and 60° (Figure 3(c)).

The average values of the mechanical parameters of the specimens are listed in Table 2. The wing crack initiation strength, σ_i, is difficult to be identified based on the stress-strain curves plotted in Figure 3. In this test, the AE hit rate curve was used to obtain the wing crack initiation strength, σ_i. The axial stress and AE hit curves of sample 45-1 with flaw inclination angle of 45° are plotted in Figure 4. The AE hit rate remained at a relatively low level during the initial loading stage. However, the AE hit rate increased sharply to 20 times per second when the axial stress reached about 18.66 MPa. Concurrently, the axial stress dropped rapidly from 18.66 MPa to 18.55 MPa. After that, a wing crack was observed to initiate from the tips of the prefabricate flaw. Therefore, the wing crack initiation strength, σ_i, of sample 45-1 was identified to be 18.66 MPa.

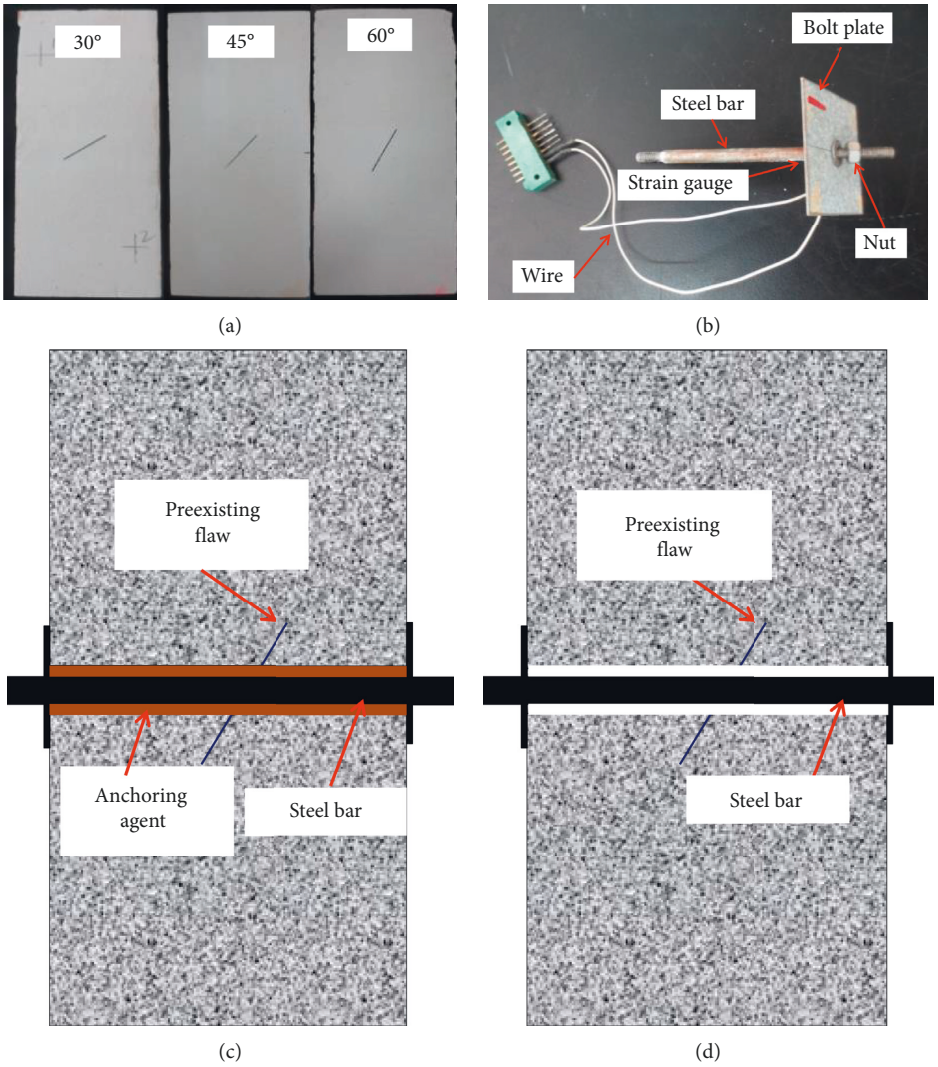

Figure 1: Geometry of the specimens and two different types of rock bolt. (a) Specimens. (b) Steel bar. (c) Fully bonded bolt. (d) Prestressed bolt.

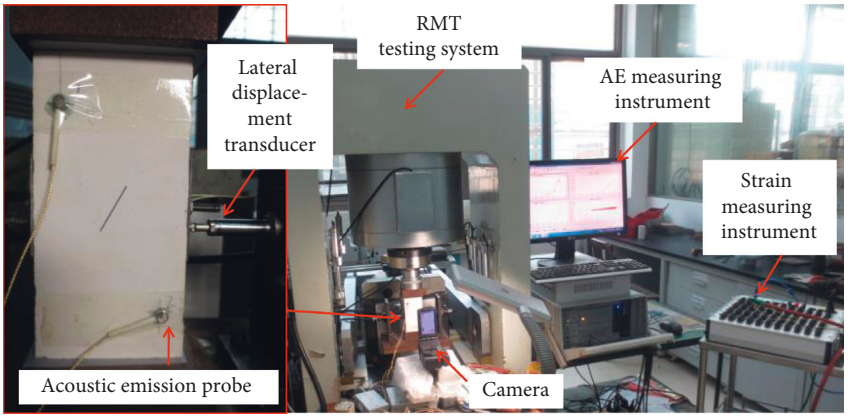

Figure 2: The testing system.

The effect of rock bolts on the mechanical parameters E, σ_i, σ_p, and σ_r of fractured specimens is shown in Figure 5, and the following conclusions can be obtained:

(1) The mechanical parameters of E, σ_i, and σ_p decreased first and then increased with an increase in the flaw inclination angle from 30° to 60° for the

Table 2: Test results of specimens under uniaxial compression.

α (°)	Group number	Type of bolt	Pretension stress (MPa)	E (GPa)	σ_i (MPa)	σ_p (MPa)	σ_r (MPa)
30	1	Unbolted	—	13.30	25.69	33.54	1.82
	2	Fully bonded	—	13.81	31.00	35.99	11.70
	3	Prestressed	36	13.67	28.23	35.97	13.75
	4	Prestressed	60	14.38	30.01	36.26	14.60
45	5	Unbolted	—	12.83	17.49	28.80	4.34
	6	Fully bonded	—	14.05	29.12	33.85	12.35
	7	Prestressed	36	13.65	20.60	32.22	17.17
	8	Prestressed	60	14.20	23.51	33.66	18.47
60	9	Unbolted	—	13.06	28.93	31.28	6.94
	10	Fully bonded	—	14.58	33.03	36.40	11.91
	11	Prestressed	36	13.96	31.31	33.75	15.85
	12	Prestressed	60	14.63	32.14	34.27	16.76

E represents the elastic modulus. σ_i is defined as the wing crack initiation strength, and σ_p is defined as uniaxial compressive strength. σ_r represents the residual strength.

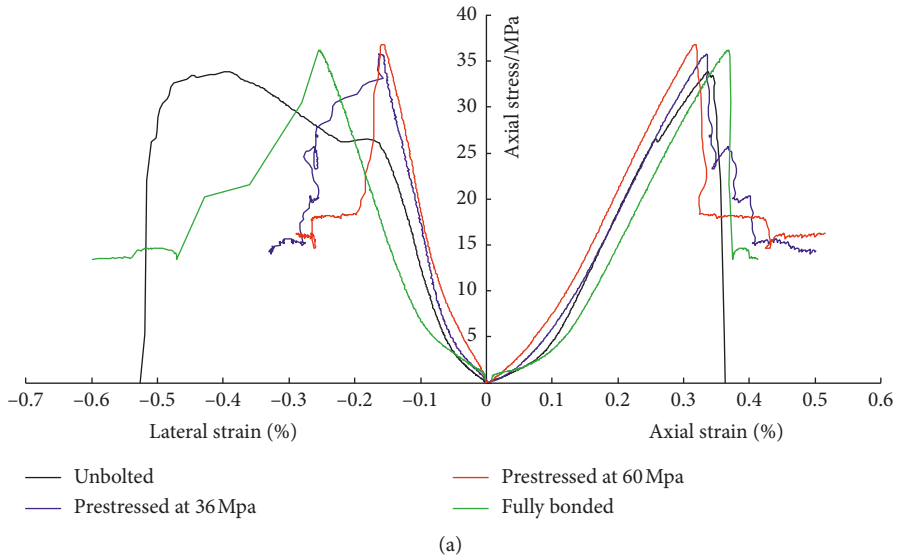

(a)

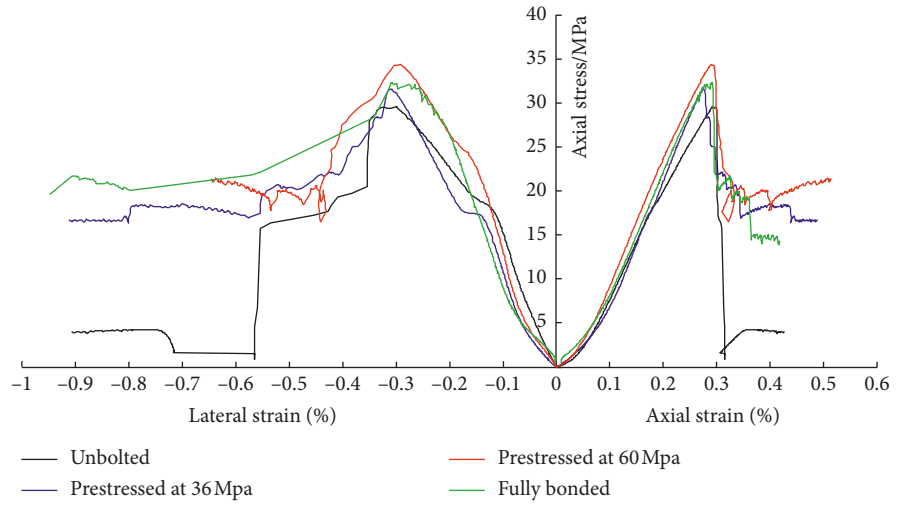

(b)

Figure 3: Continued.

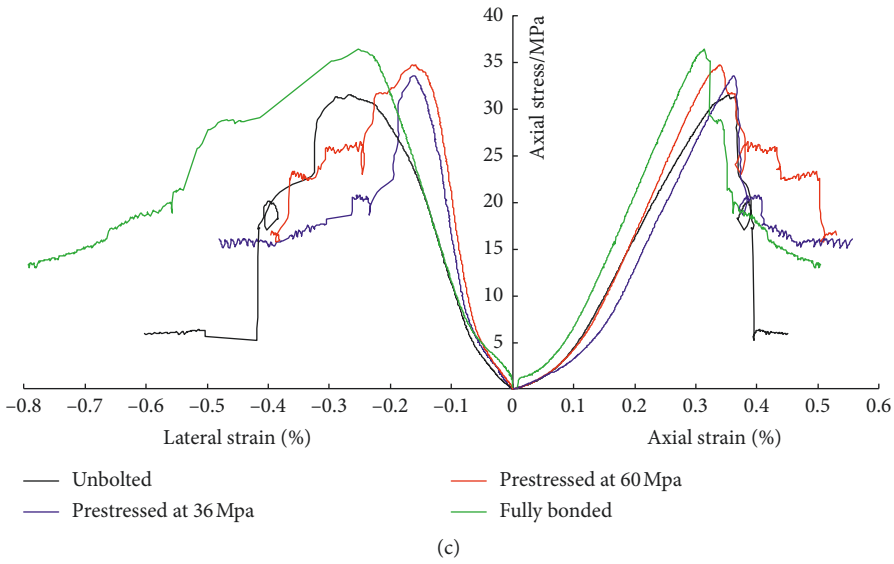

Figure 3: Typical stress-strain curves of specimens under uniaxial compression. (a) $\alpha = 30^{\circ}$. (b) $\alpha = 45^{\circ}$. (c) $\alpha = 60^{\circ}$.

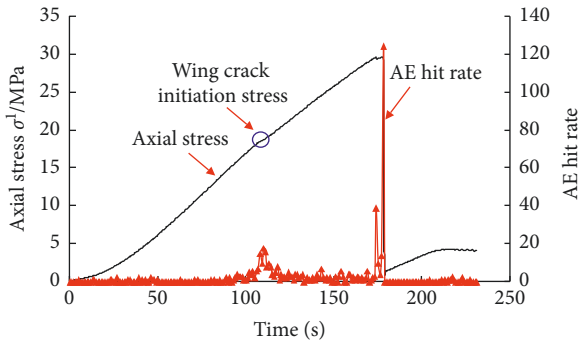

Figure 4: Relation between axial stress, AE hit rate, and time of sample 45-1.

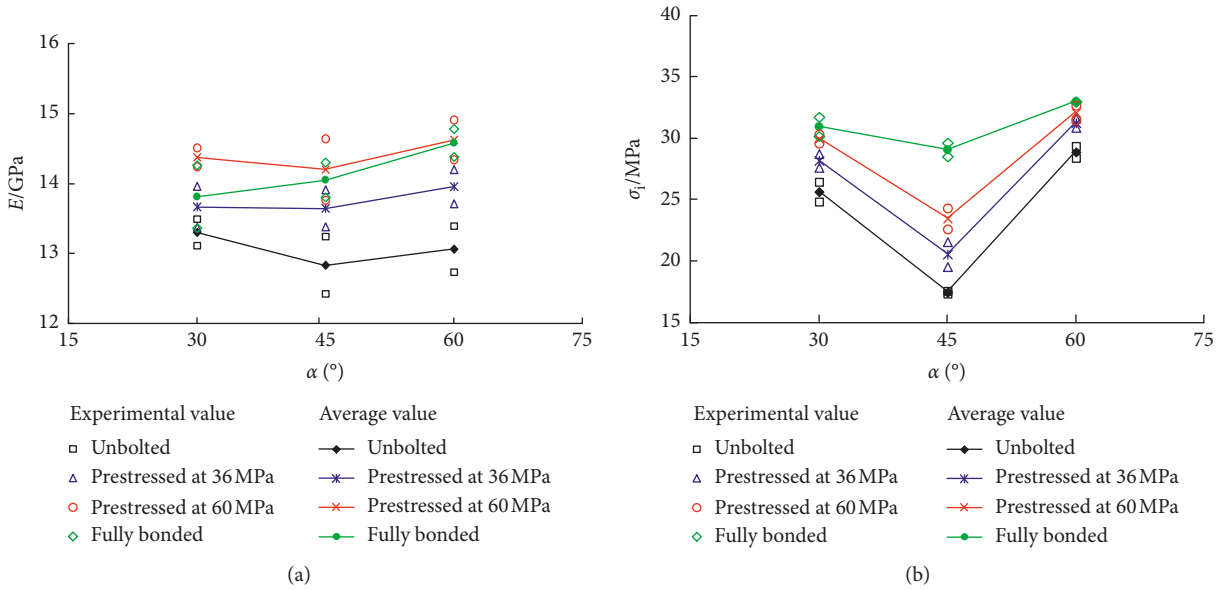

Figure 5: Continued.

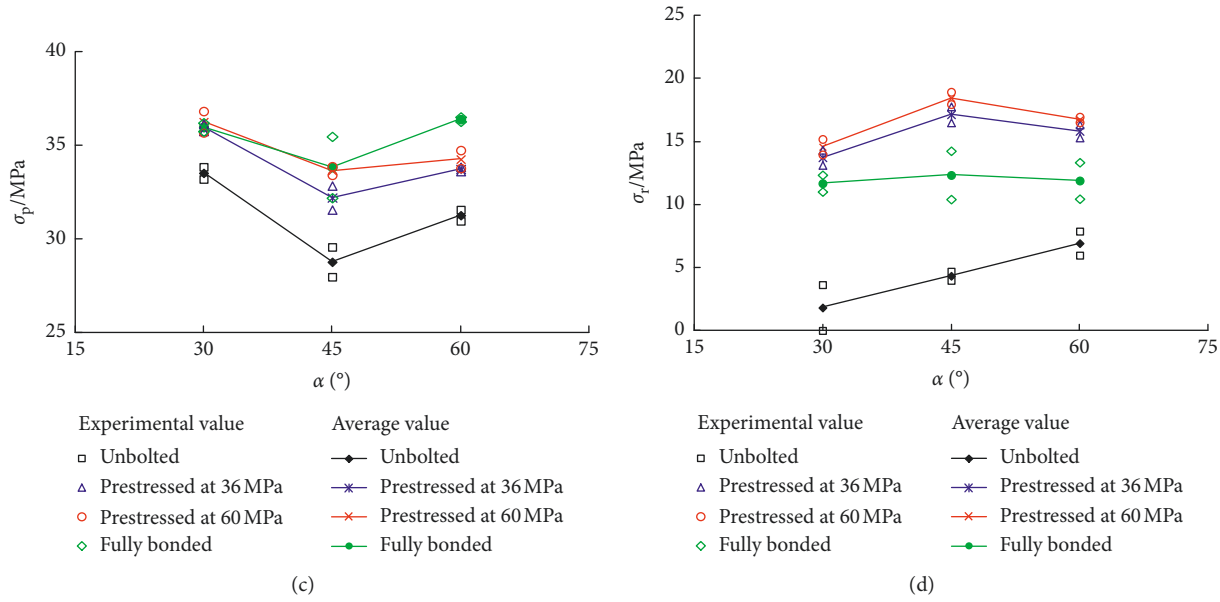

Figure 5: The effect of the two types of bolts on the mechanical parameters of specimens. (a) Elastic modulus. (b) Wing crack initiation strength. (c) Uniaxial compressive strength. (d) Residual strength.

unbolted specimens. The minimum value of these parameters was obtained at 45°. These variations are consistent with previous research results [28–31].

(2) The average E, σ_i, σ_p, and σ_r of specimens with different flaw inclination angles all increased due to the effect of the rock bolt. The increase in residual strength, σ_r, was the most significant among all the mechanical parameters.

(3) For the fractured specimens anchored with a prestressed bolt or a fully bonded bolt, the increase degree of the mechanical parameters σ_i and σ_p was the greatest for the specimens with flaw inclination angles of 45°. Taking the fractured specimens anchored with a fully bonded bolt as example, as α increased from 30° to 60°, the average value of σ_i increased by 20.67%, 66.49%, and 14.17%, respectively, and σ_p increased by 7.31%, 17.53%, and 16.37%, respectively.

(4) The mechanical parameters E, σ_i, σ_p, and σ_r of specimens anchored with a prestressed bolt increased with an increase in pretension stress. For example, the average value of E, σ_i, σ_p, and σ_r increased by 4.03%, 14.13%, 4.47%, and 7.57%, respectively, with an increase in pretension stress from 36 MPa to 60 MPa for specimens with flaw inclination angle of 45°.

(5) The reinforcement effect of the two types of rock bolts was different for different mechanical parameters. The fully bonded bolt was superior to the prestressed bolt with respect to increasing σ_i of specimens. However, the prestressed bolt was more efficient than the fully bonded bolt with respect to increasing σ_r of fractured specimens.

3.2. Typical Failure Modes

3.2.1. Unbolted Specimens. Typical failure modes of unbolted specimens are shown in Figure 6 (T stands for tensile crack, S stands for shear crack, and the grey area represents surface spalling). The cracking process of unbolted specimen can be described as follows. A tensile wing crack first initiated from the tip of the flaw and then propagated in a stable manner along the direction of axial stress. As the load increased, a secondary crack initiated from the tip of the flaw and propagated along a coplanar plane along the flaw in a stable manner. When the loads reached near peak strength, unstable failure occurred accompanied by an obvious shear movement, generally along the plane of the preexisting flaw. After tests, as shown in Figure 7, the unbolted sample can be easily forced apart with hands into two parts along the macroscopic fracture surface of secondary shear crack.

3.2.2. Specimens Anchored with Prestressed Bolt. Although the cracking process of the bolted specimens was similar to that of the unbolted specimens, a comparison of Figures 6 and 8 reveals some different failure characteristics between them.

(1) For the specimens anchored with the prestressed bolt, opening displacement between the two fracture surfaces of the tensile wing crack was greatly suppressed. The propagation path of the wing crack was difficult to clearly identify in the samples with flaw inclination angles of 30° (Figure 8(a)) and 60° (Figure 8(c)).

(2) Macroscopic fractures propagating through the entire sample did not occur because of the effect of the rock bolt. Furthermore, the fractured sample

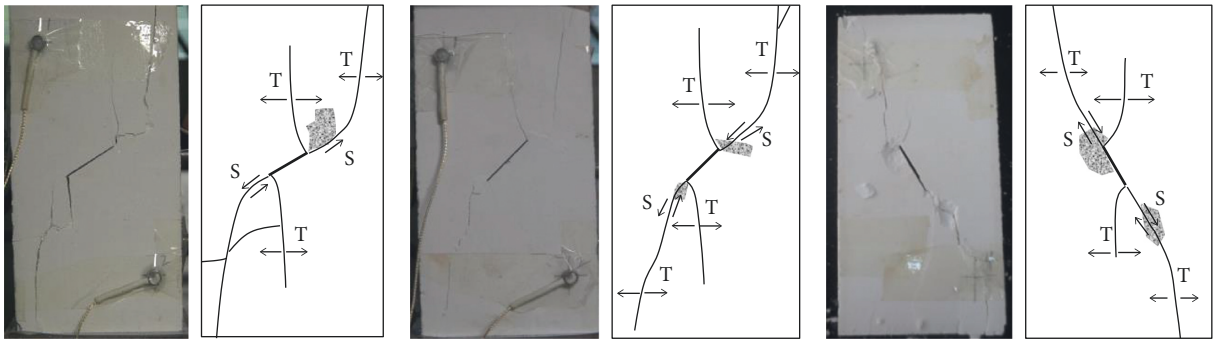

(a) (b) (c)

Figure 6: Failure modes of unbolted specimens containing flaws with different inclination angles. (a) $\alpha = 30^{\circ}$. (b) $\alpha = 45^{\circ}$. (c) $\alpha = 60^{\circ}$.

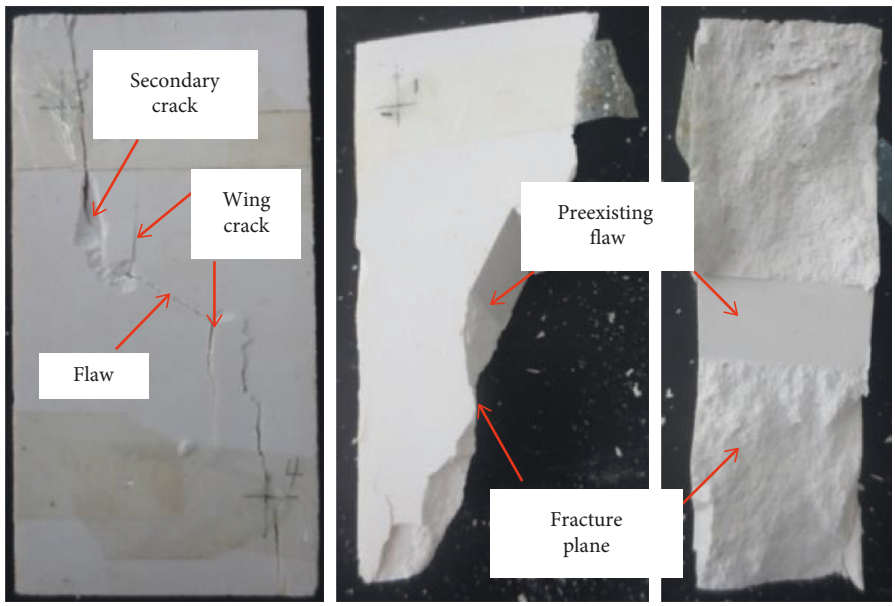

Figure 7: Macroscopic fracture in the unbolted sample.

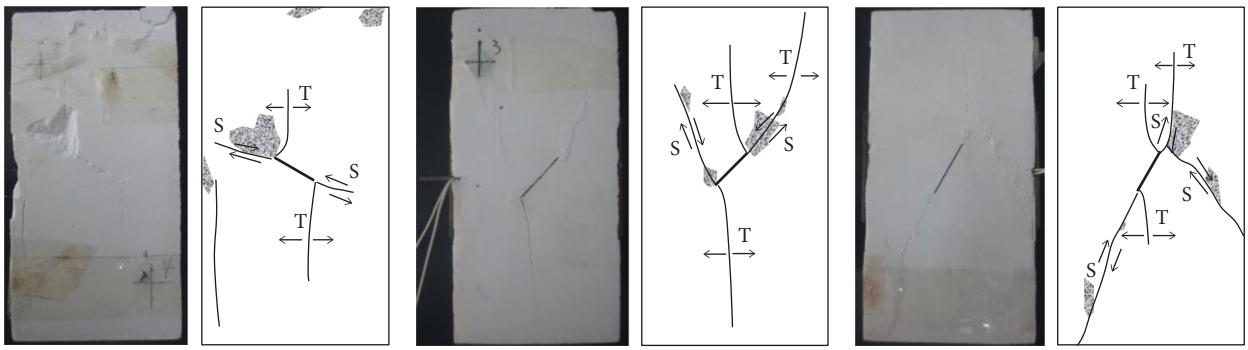

(a) (b) (c)

Figure 8: Failure modes of specimens anchored with prestressed bolt. (a) $\alpha = 30^{\circ}$. (b) $\alpha = 45^{\circ}$. (c) $\alpha = 60^{\circ}$.

was reinforced by the bolt and could not be easily forced apart by hand. This was the main reason why the residual strength of the specimens anchored with the prestressed bolt improved significantly.

3.2.3. Specimens Anchored with Fully Bonded Bolt. Failure modes of specimens anchored with the fully bonded bolt are shown in Figure 9. When the sample is anchored with the fully bonded bolt, the secondary crack does not penetrate the whole sample. In addition, although the

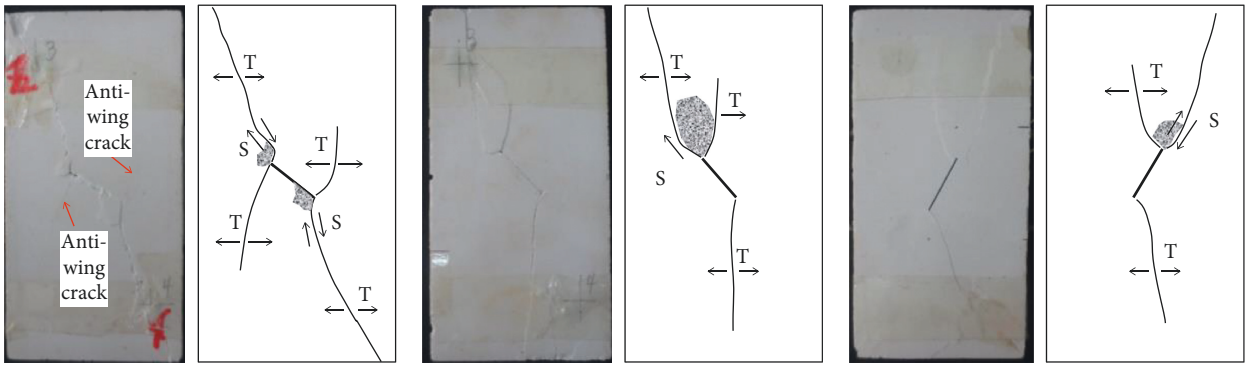

Figure 9: Failure modes of specimens anchored with fully bonded bolt. (a) $\alpha = 30^{\circ}$. (b) $\alpha = 45^{\circ}$. (c) $\alpha = 60^{\circ}$.

initiation and propagation of wing cracks occurred in the bolted sample, due to the restraint effect of the bolt, the separation displacement between the two surfaces of tensile wing crack is greatly suppressed and the propagation path of wing crack is difficult to be identified. Therefore, the bolted sample maintains a good integrity.

It is important to note that for the specimens anchored with the fully bonded bolt with flaw inclination angle of 30°, the cracking mechanism is different with unbolted samples. Anti-wing crack instead of wing crack initiated from the tips of preexisting flaw is plotted in Figure 9(a). Unlike the wing crack, the formation mechanism of the anti-wing crack is more complicated. In this test, the fully bonded bolt directly interacts with the preexisting crack through the anchoring agent; this may be the main formation mechanism of the anti-wing crack. Under the action of the fully bonded bolt, the formation mechanism of anti-wing cracks needs to be further studied.

3.3. Tension Stress in the Prestressed Bolt. Tension stress in the rock bolt is closely related to the deformation and failure process of the specimen, so an analysis of tension stress is of great significance to understand the working mechanism of the rock bolt. Variation of tension stress in the prestressed bolt during the loading process was divided into three different stages, as shown in Figure 10.

(1) Stage A: slow growth stage. Elastic deformation occurred during the early loading period, and the lateral deformation of the sample increased at a low rate. As a result, the tension stress in the prestressed bolt increased slowly with time.

(2) Stage B: stable growth stage. Wing crack initiated at the beginning of this stage, after which the tension stress of the bolt increased abruptly and then entered a stable growth stage. In this stage, the separation displacement between the two surfaces of the wing crack gradually increased, leading to a steady growth of the tension stress in the rock bolt.

(3) Stage C: rapid growth stage. The tension stress in the bolt increased abruptly again after peak strength. During this stage, a macroscopic fracture had developed, and the separation deformation of the fractured sample further increased under the axial load. The tension stress increased at a relatively large rate due to the restriction effect of the bolt on specimen deformation. Finally, the tension stress in the bolt reached the peak value when the bearing capacity of the sample no longer decreased.

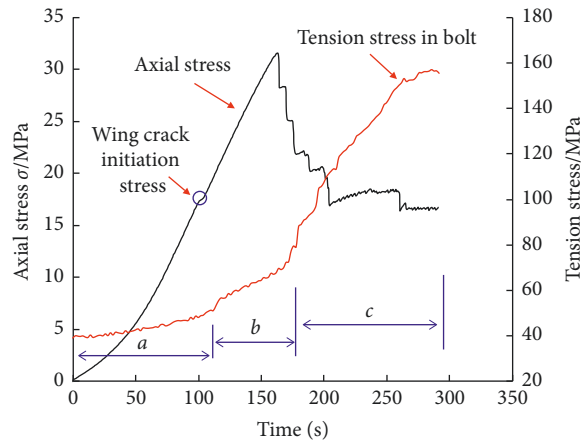

Figure 10: Tension stress in the bolt for the sample with flaw inclination angle of 45° with pretension stress of 36 MPa.

For the specimens with flaw inclination angles of 30° and 60°, the variation of tension stress in the rock bolts were very similar to that of specimen with flaw inclination angle of 45°. However, the peak tension stress values were different, as shown in Figure 11. With an increase in the inclination angle from 30° to 60°, the peak tension stress value first increased and then decreased and obtained the maximum value at inclination angle of 45°. Besides, the peak tension stress value increased with pretension stress. For example, with an increase of pretension stress from 36 MPa to 60 MPa, the peak tension stress value increased from 82.14 MPa to 126.26 MPa for specimens with flaw inclination angle of 30°.

4. Discussion

In Section 3.1, we concluded that the fully bonded bolt was superior to the prestressed bolt with respect to increasing σ_i,

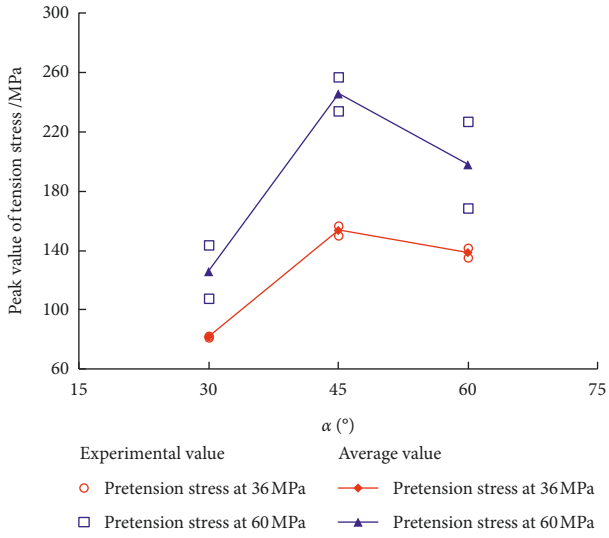

Figure 11: Peak tension stress value in the bolt for samples with different flaw inclination angles.

and the prestressed bolt was more efficient than the fully bonded bolt with respect to increasing σ_r of fractured specimens. Due to the limited number of samples, only two different pretension stress values, i.e., 36 MPa and 60 MPa, were used for this test. If the pretension stress of the prestressed bolt was set to a value less than 36 MPa or a value greater than 60 MPa, the above conclusion may not be correct. Further experimental research is needed to validate this conclusion.

Based on the analysis of experimental results in Section 3.2, we can conclude that an increase in the pretension stress can improve the anchoring effect of prestressed bolts on fractured rock. However, as analyzed in Section 3.3, a higher pretension stress will result in a larger peak tension stress value. In other words, tensile failure of the bolt can occur if the pretension stress is set too high. The experimental results provide some useful guidance for the design of bolt support in engineering. The pretension stress of rock bolts should be set to a reasonable value, which will not only improve the anchoring effect on the surrounding rock but also avoid the tensile failure of the bolt.

5. Conclusions

Uniaxial compression tests were conducted to investigate the anchoring effect of two different types of bolts on specimens containing a single flaw with different inclination angles. Based on the analysis of experimental results, primary conclusions are summarized as follows.

Both the prestressed and fully bonded bolt had a significant influence on the mechanical behavior of the fractured rock. The drop rate of axial stress significantly reduced and lateral deformation was significantly inhibited after peak strength for the bolted specimens.

The average value of E, σ_i, σ_p, and σ_r of bolted specimens all increased due to the effect of the rock bolt. The increase degree was the greatest for the specimens with flaw inclination angle of 45°. The increase in residual strength, σ_r, was the most significant among all the mechanical parameters. Besides, the mechanical parameters of specimens anchored with a prestressed bolt increased with an increase in pretension stress.

The reinforcement effect of the two types of rock bolts was different for different mechanical parameters. The fully bonded bolt was superior to the prestressed bolt with respect to increasing σ_i of specimens. However, the prestressed bolt was more efficient than the fully bonded bolt with respect to increasing σ_r of fractured specimens.

The bolted specimens displayed different failure characteristics compared to the unbolted specimens. Opening displacement was greatly suppressed between the two surfaces of the tensile wing crack. The fractured sample was reinforced by the bolt, and macroscopic fractures propagating through the entire sample did not occur.

Variation of tension stress in the prestressed bolt during the loading process was divided into three different stages: a slow growth stage, a stable growth stage, and a rapid growth stage. With an increase in the inclination angle from 30° to 60°, the peak tension stress value first increased and then decreased and obtained the maximum value at inclination angle of 45°. Besides, the peak tension stress value increased with pretension stress.

Data Availability

The data used to support the findings of this study are available from the corresponding author upon request.

Conflicts of Interest

The authors declare that there are no conflicts of interest regarding the publication of this paper.

Acknowledgments

The authors would like to acknowledge the financial support provided by the National Natural Science Foundation of China (grant no. 51709113) and the Science and Technology Project of Henan Province (grant no. 172102310475).

References

[1] N. Bahrani and J. Hadjigeorgiou, "Explicit reinforcement models for fully-grouted rebar rock bolts," *Journal of Rock Mechanics and Geotechnical Engineering*, vol. 9, no. 2, pp. 267–280, 2017.

[2] L. St-Pierre, F. P. Hassani, P. H. Radziszewski, and J. Ouellet, "Development of a dynamic model for a cone bolt," *International Journal of Rock Mechanics and Mining Sciences*, vol. 46, no. 1, pp. 107–114, 2009.

[3] M. Cai and D. Champaigne, "Influence of bolt-grout bonding on MCB conebolt performance," *International Journal of Rock Mechanics and Mining Sciences*, vol. 49, pp. 165–175, 2012.

[4] W. D. Orelepp, J. J. Bornman, and N. Erasmus, "The durabara yieldable support tendon-design rationale and laboratory results," in *Rockbursts and Seismicity in Mines*, pp. 263–266, South African Inst of Mining and Metallurgy, Johannesburg, South Africa, 2001.

[5] C. C. Li, "A new energy-absorbing bolt for rock support in high stress rock masses," *International Journal of Rock Mechanics and Mining Sciences*, vol. 47, no. 3, pp. 396–404, 2010.

[6] C. C. Li, "Performance of D-bolts under static loading," *Rock Mechanics and Rock Engineering*, vol. 45, no. 2, pp. 183–192, 2011.

[7] C. C. Li and C. Doucet, "Performance of D-bolts under dynamic loading," *Rock Mechanics and Rock Engineering*, vol. 45, no. 2, pp. 193–204, 2011.

[8] A. Doucet, "Laboratory testing of a new type of energy absorbing rock bolt," *Tunnelling and Underground Space Technology*, vol. 20, no. 4, pp. 291–300, 2005.

[9] M. He, W. Gong, and J. Wang, "Development of a novel energy-absorbing bolt with extraordinarily large elongation and constant resistance," *International Journal of Rock Mechanics and Mining Sciences*, vol. 67, pp. 29–42, 2014.

[10] W. D. Ortlepp and T. R. Stacey, "Rockburst mechanisms in tunnels and shafts," *Tunnelling and Underground Space Technology*, vol. 9, no. 1, pp. 59–65, 1994.

[11] T. R. Stacey, W. D. Ortlepp, and H. Kirsten, "Energy-absorbing capacity of reinforced shotcrete, with reference to the containment of rockburst damage," *Journal of the Southern African Institute of Mining and Metallurgy*, vol. 95, no. 3, pp. 137–140, 1995.

[12] P. K. Kaiser, D. D. Tannant, and D. R. McCreath, *Canadian Rockburst Support Hand-Book, Geomechanics Research Centre*, Laurentian University, Sudbury, Ontario, Canada, 1996.

[13] W. D. Ortlepp and T. R. Stacey, "Performance of tunnel support under large deformation static and dynamic loading," *Tunnelling and Underground Space Technology*, vol. 13, no. 1, pp. 15–21, 1998.

[14] C. Zhang, X.-T. Feng, H. Zhou, S. Qiu, and W. Wu, "Case histories of four extremely intense rockbursts in deep tunnels," *Rock Mechanics and Rock Engineering*, vol. 45, no. 3, pp. 275–288, 2012.

[15] F. Meng, L. N. Y. Wong, H. Zhou et al., "Shear rate effects on the post-peak shear behaviour and acoustic emission characteristics of artificially split granite joints," *Rock Mechanics and Rock Engineering*, pp. 1–20, 2019.

[16] H. Zhou, F. Meng, C. Zhang, D. Hu, F. Yang, and J. Lu, "Analysis of rockburst mechanisms induced by structural planes in deep tunnels," *Bulletin of Engineering Geology and the Environment*, vol. 74, no. 4, pp. 1435–1451, 2014.

[17] C. Li and B. Stillborg, "Analytical models for rock bolts," *International Journal of Rock Mechanics and Mining Sciences*, vol. 36, no. 8, pp. 1013–1029, 1999.

[18] Y. Cai, T. Esaki, and Y. Jiang, "An analytical model to predict axial load in grouted rock bolt for soft rock tunnelling," *Tunnelling and Underground Space Technology*, vol. 19, no. 6, pp. 607–618, 2004.

[19] Y. Cai, T. Esaki, and Y. Jiang, "A rock bolt and rock mass interaction model," *International Journal of Rock Mechanics and Mining Sciences*, vol. 41, no. 7, pp. 1055–1067, 2004.

[20] K. Spang and P. Egger, "Action of fully-grouted bolts in jointed rock and factors of influence," *Rock Mechanics and Rock Engineering*, vol. 23, no. 3, pp. 201–229, 1990.

[21] A. Kılıc, E. Yasar, and A. G. Celik, "Effect of grout properties on the pull-out load capacity of fully grouted rock bolt," *Tunnelling and Underground Space Technology*, vol. 17, no. 4, pp. 355–362, 2002.

[22] G. Grasselli, "3D behaviour of bolted rock joints: experimental and numerical study," *International Journal of Rock Mechanics and Mining Sciences*, vol. 42, no. 1, pp. 13–24, 2005.

[23] S. C. Li, N. Zhang, A. Z. Lu, M. T. Li, and L. Yang, "Experimental study of anchoring effect of discontinuous jointed rock mass under uniaxial tension," *Chinese Journal of Rock Mechanics and Engineering*, vol. 30, no. 8, pp. 1579–1586, 2011.

[24] B. Zhang, S. Li, and K. Xia, "Reinforcement of rock mass with cross-flaws using rock bolt," *Tunnelling and Underground Space Technology*, vol. 51, pp. 346–353, 2016.

[25] A. M. Ferrero, "The shear strength of reinforced rock joints," *International Journal of Rock Mechanics and Mining Sciences & Geomechanics Abstracts*, vol. 32, no. 6, pp. 595–605, 1995.

[26] Y. Chen and C. C. Li, "Experimental and three-dimensional numerical studies of the anchorage performance of rock bolts," in *Proceedings of the 13th International Congress of Rock Mechanics*, Montreal, Canada, 2015.

[27] C. C. Li, "A practical problem with threaded rebar bolts in reinforcing largely deformed rock masses," *Rock Mechanics and Rock Engineering*, vol. 40, no. 5, pp. 519–524, 2006.

[28] A. Bobet and H. H. Einstein, "Fracture coalescence in rock-type materials under uniaxial and biaxial compression," *International Journal of Rock Mechanics and Mining Sciences*, vol. 35, no. 7, pp. 863–888, 1998.

[29] R. H. C. Wong, K. T. Chau, C. A. Tang, and P. Lin, "Analysis of crack coalescence in rock-like materials containing three flaws-Part I: experimental approach," *International Journal of Rock Mechanics and Mining Sciences*, vol. 38, no. 7, pp. 909–924, 2001.

[30] L. N. Y. Wong and H. H. Einstein, "Systematic evaluation of cracking behavior in specimens containing single flaws under uniaxial compression," *International Journal of Rock Mechanics and Mining Sciences*, vol. 46, no. 2, pp. 239–249, 2009.

[31] C. H. Park and A. Bobet, "Crack coalescence in specimens with open and closed flaws: a comparison," *International Journal of Rock Mechanics and Mining Sciences*, vol. 46, no. 5, pp. 819–829, 2009.